ACS Sustainable Chemistry & Engineering

Research Article

pubs.acs.org/journal/ascecg

Biomimetically Synthesized Hierarchical TiO_2-Graphitic Carbon as Anodic Catalysts for Direct Alkaline Sulfide Fuel Cell

Prakash Chandra Sahoo,[†] Kwiyong Kim,[‡] Jay Hyung Lee,*[,§] Jong-In Han,*[,‡] and You-Kwan Oh[∥]

[†]Centre for Nano Science and Nano Technology, Institute of Technical Education and Research, Siksha 'O' Anusandhan University, Bhubaneswar-751030, India

[‡]Department of Civil and Environmental Engineering, Korea Advanced Institute of Science and Technology (KAIST), 291 Daehak-ro, Yuseong-gu, Daejeon 305-701, Republic of Korea

[§]Department of Chemical and Biomolecular Engineering, Korea Advanced Institute of Science and Technology (KAIST), 291 Daehak-ro, Yuseong-gu, Daejeon 305-701, Republic of Korea

[∥]Biomass and Waste Energy Laboratory, Korea Institute of Energy Research (KIER), 152 Gajeong-ro, Yuseong-gu, Daejeon 305-343, Republic of Korea

ABSTRACT: TiO_2-graphitic carbon composites (TiO_2/G) with hierarchical structures were synthesized using microalgae cells as the biotemplate and then applied as the anode catalyst for a promising sulfide-based fuel cell, named direct alkaline sulfide fuel cell (DASFC). The results of X-ray diffraction, Raman spectroscopic analysis, morphology, nitrogen adsorption−desorption studies, and X-ray photoelectron spectroscopy demonstrated a networked nanostructure with high specific surface area. This novel TiO_2/G composite, possessing a notably wide surface area, exhibited strong catalytic activity in alkaline sulfide oxidation, with the highest maximum power density of 38.90 mW cm^{-2} obtained with 60 wt % TiO_2/G at 70 °C. The present results demonstrated that TiO_2/G has a great potential to be used as powerful and economical anode catalysts for a DASFC.

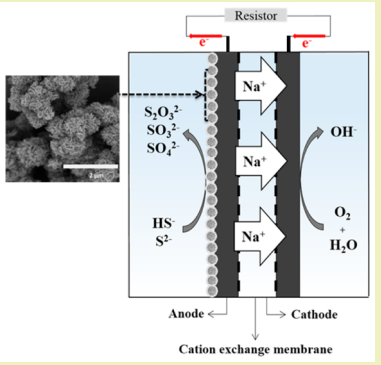

KEYWORDS: *Titanium dioxide, Biotemplate, Microalgae, Direct alkaline sulfide fuel cell, Anode catalyst*

INTRODUCTION

Hydrogen sulfide (H_2S), existing in various crude gases, such as natural gas, shale gas, and biogas, is known to be corrosive and toxic. For the sake of air quality management, treatment of this detriment gas should be carried out before emission to the air. The best known technology for this sweetening purpose named the "Claus process", though widely used, is questionable for its sustainability issue because the reactor itself is largely complicated, and operational conditions are harsh.[1] In addition, a major byproduct hydrogen, which potentially lowers the overall economic burden if well used, is in vain due to impurities such as CS_2, SO_2, and COS.[2] It is therefore of necessity to develop more feasible alternatives that enable the efficient removal of H_2S and better still harvest energy during operation.[1,2]

Fuel cell-based treatment is one such approach. In this strategy, gaseous/aqueous sulfide is oxidized as a fuel with electrical power generated while being converted to sulfur or more oxidized species.[3−6] Among various types of sulfide-fed fuel cells reported so far, the direct alkaline sulfide fuel cell (DASFC) is one most suited in terms of mild operation conditions compared to other types[3−6] and especially with no sulfur deposition on the anode.[7] When extracting electricity from a waste-derived liquid fuel (i.e., aqueous sulfide solution), which is cheap even with easiness in storage and transportation, DASFC can serve as a functional fuel cell, which is aimed at not only gas sweetening but also power generation.

The anodic reactions in DASFC are as follows:

First, sulfide electro-oxidation to elemental sulfur is dominant:[1,2]

$$HS^- + OH^- \rightarrow S + H_2O + 2e^-;\ E^0 = -0.478\ \text{V vs SHE} \quad (1)$$

$$S^{2-} \rightarrow S + 2e^-;\ E^0 = -0.508\ \text{V vs SHE} \quad (2)$$

Thus, formed sulfur then combines with sulfide/polysulfide to form (longer) polysulfide:[1,2]

$$HS^- + (n-1)S^0 + OH^- \rightarrow {S_n}^{2-} + H_2O;\ n = 2-5 \quad (3)$$

$${S^0} + {S_n}^{2-} \rightarrow {S_{n+1}}^{2-};\ n = 2-4 \quad (4)$$

The final fate of the anodic process is the formation of sulfur oxyanions from electro-oxidation of sulfide/polysulfide:[1,7]

$$S^{2-} + 6OH^- \rightarrow {SO_3}^{2-} + 3H_2O + 6e^-;\ E^0 = -0.597\ \text{V vs SHE} \quad (5)$$

Received: April 5, 2015
Revised: June 20, 2015
Published: June 29, 2015

DOI: 10.1021/acssuschemeng.5b00277
ACS Sustainable Chem. Eng. 2015, 3, 1764−1770

$$S_n^{2-} + 6OH^- \rightarrow S_2O_3^{2-} + 3H_2O + (n-2)S + 6e^-;$$
$$n = 2 - 5;$$
$$E^0 = -0.647 \text{ V vs SHE} \quad (6)$$

Unfortunately, the fuel cell performance, albeit the high electrochemical activity of the fuel sulfide itself, is not yet satisfactory especially in the absence of an anode catalyst. The main focus of recent investigations on DASFC is therefore to accelerate the anodic kinetics with the aid of an electrocatalyst and, if possible, with the minimal use of expensive metals. For instance, various compounds such as metal sulfides[8] and heteropolyacids[9] have been reported to produce quite meaningful power output. Bimetallic alloys are other promising candidates; it was found that bimetallic palladium−cobalt or palladium−iridium showed higher activity than Pd itself and especially the widely active noble metal Pt.[10−12] However, the performance of the anodic catalyst, which is in fact an essential condition, needs to be further improved in order to meet the economical aspects for the implementation of the DASFC-based H_2S capture technology.

Nanostructured materials with hierarchical morphology and large specific surface area could offer one reasonable direction for such an endeavor, as they are bound to have highly enhanced electron-transfer rates.[13] Among various ways to prepare such nanomaterials, biotemplateing, which is to fabricate nanosized structures using microbes as templates, is considered to be a green and economical option.[14] Biotemplates often exhibit precise widths and lengths, complex exterior and interior surfaces, and uniform geometries, all of which have inspired researchers to produce multiscale hybrid inorganic materials that exhibit surprising morphologies.[15]

In this work, we present a simple and one-pot route to synthesize TiO_2-graphitic carbon composites (TiO_2/G) using microalgae (*Chlorellasp.* KR-1[16]), whose cells have spherical shapes with average diameters of 2 μm, as the biotemplate. The use of microalgae has two distinct advantages: (i) The negative charged cells can function both as a structure directing agent and a natural source of graphitic carbon. (ii) It can be prepared at low cost even on a large scale. The TiO_2/G composite is expected to have the unique advantages of high surface area and improved electronic conductivity in contrast to pure TiO_2. Hence, we envisage the use of the TiO_2/G hybrid as anodic catalysts for DASFC application. To the best of our knowledge, this new hybrid composite was fabricated and applied to DASFC for the first time.

RESULTS AND DISCUSSION

Physicochemical Characterization of Hierarchical TiO_2/G Hybrid. The synthesis of hierarchical TiO_2/G microspheres using the microalgae template was carried out in a simple one-pot method. First, microalgae cells (*Chlorella* sp. KR-1) were concentrated by centrifugation and washed in deionized water to remove the spent medium, and then they were dispersed in ethanol. A stoichiometric amount of titanium isopropoxide was added, followed by the addition of a small amount of water. At this stage, titanium isopropoxide underwent hydrolysis and formed titanium tetrahydroxide, which experienced coordination expansion on the surface of microalgae.[17] Heat treatment of the obtained material was carried out at 400 °C under an Ar atmosphere. With a gradual increase in temperature, metallic crystal growth occurred, and the grown metal became embedded into the graphitic carbon matrix of the microalgae. The morphologies of thus-formed TiO_2/G composites were observed using SEM (Figure 1). Hierarchical worm-like TiO_2/G microstructures were found in the presence of microalgae as the template with the size of the microstructures ranging from 1 to 2 μm. However, in the absence of microalgae, rigid spherical TiO_2 crystals were obtained. This result confirmed that the microalgae surface played a key role in controlling the morphology of the TiO_2/G composite. From FETEM observation (Figure 1g), it was observed that nanosized TiO_2 crystals were embedded in the graphitic matrix.

Phases of the synthesized TiO_2/G composite were determined by X-ray diffraction. Figure 2a displays the characteristic patterns of TiO_2, and the main peaks (25° (101), 48° (200), 53° (105), 55° (211) and 63° (204)) can be indexed to the anatase TiO_2 phase (JCPDS, card no. 21-1272).[18] Furthermore, the two broad peaks of graphitic carbon obtained from the microalgae sample at around 25° and 44° can be indexed as a graphite carbon framework. The patterns of the TiO_2/G composites indicated that with an increasing content of TiO_2 in the sample, the peaks of the anatase form of TiO_2 became stronger. Further, it was concluded that the graphitic carbon had no effect on the crystallization characteristics of TiO_2.

Raman spectra were employed to further confirm the crystalline phase of TiO_2 and the existence of carbon in the TiO_2/G composite (Figure 2b). The five Raman modes with strong intensities at 145, 196, 395, 515, and 635 cm^{-1} are seen in all the samples, which are in good agreement with the typical Raman features of anatase TiO_2 phase and confirm that TiO_2 is in anatase phase. The two characteristic peaks located at about 1372 and 1592 cm^{-1} in the Raman spectrum of the TiO_2/G nanosphere correspond to the D-band and G-band of carbon, respectively. The low peak integrated intensity of the D-band to G-band indicates the existence of a disordered carbon structure, which is consistent with the above XRD results.[18]

The results of the specific surface area of different wt % TiO_2/G composites are shown in Figure 2c−f. The hierarchically porous composites with different wt % of TiO_2 had BET surface areas in the range of 158.2−372.8 $m^2\ g^{-1}$. On the other hand, TiO_2 formed in the absence of microalgae had a specific surface area of 8.0 $m^2\ g^{-1}$, which is much less than that of the TiO_2/G composite. This substantially enhanced surface area was one distinctive advantage of the algae-template composite material, given that high specific surface area is one of the most critical factors in relation to the activity of the electrode materials. The rate of fuel conversion is a function of the active sites of an electrode and/or catalyst on which the substrate can reacts.

The electronic environment of the TiO_2/G composite was confirmed using X-ray photoelectron spectroscopy (XPS). As shown in the survey spectra of the 60 wt % TiO_2/G, C 1s, O 1s, and Ti 2p peaks were detected. The Ti 2p spectrum (Figure 3b) for TiO_2/G comprises two symmetrical peaks with binding energies at 459.4 and 465.1 eV, which are attributable to Ti 2p3/2 and Ti 2p1/2, respectively. The separation between these two peaks is 5.7 eV, slightly larger than the energy splitting reported for neat TiO_2. This may be due to the encapsulation of TiO_2 in graphitic carbon.[19] As shown in Figure 3c, the O 1s binding energy (BE) at 530.5 eV may be attributed from TiO_2, while the peak at 531.6 eV may possibly originate from alcohol or adsorbed H_2O, which is in good accordance with the fitted C 1s peaks. Figure 3d displays the high resolution spectrum of the C 1s region of the as-prepared TiO2/G composite fitted to two peaks. The large peak at 284.3 eV is attributed to graphitic carbon, while the peak at 285.1 eV can be assigned to disordered carbon or oxidant carbon, such as in alcohols or hydrocarbons.[20,21] From a

DOI: 10.1021/acssuschemeng.5b00277
ACS Sustainable Chem. Eng. 2015, 3, 1764−1770

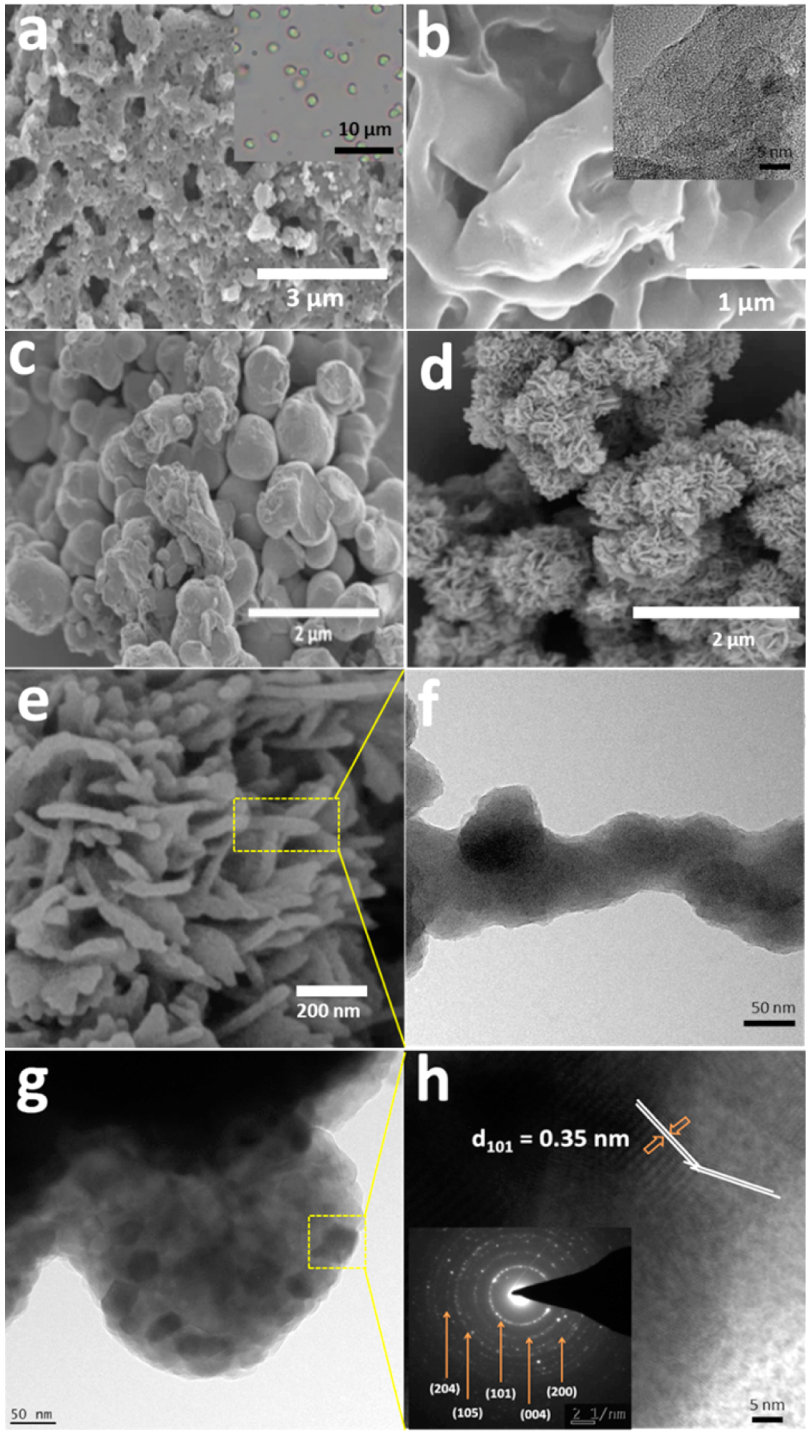

Figure 1. FESEM and FETEM image of (a) graphitic carbon from microalgae pyrolysis; inset represents an optical image of microalgae (*Chlorella* sp. KR-1), (b) enlarged image of a; inset represents FETEM image of graphitic carbon from microalgae, (c) TiO_2 synthesized without microalgae, (d) 60 wt % TiO_2/G composite synthesized using microalgae as template, (e) enlarged image of d, (f) FETEM image of worm-like structures in 60 wt % composite, (g) FETEM image of a tip 60 wt % TiO_2/G; it was clearly observed that nano-sized TiO_2 was embedded in a graphitic carbon, and (h) high resolution image of 60 wt % TiO_2/G showing the d_{100} crystal plane; inset represents the SAED patterns arising from the anatase phase of TiO_2.

combination of the FE-SEM, TEM, XRD, Raman, BET surface area, and XPS results, it is concluded that the TiO_2-graphitic carbon composites (TiO_2/G) consist of a TiO_2 crystal core inside the shell of graphitic carbon. In addition, the hierarchical 3D microstructures in the sample favor the enhancement of the electrochemical performance of the electrode.

Catalytic Behavior of TiO_2/G Composite Anode in DASFC. The CV scan of the 60 wt % TiO_2/G sample in 1 M Na_2S + 3 M NaOH is shown in Figure 4. The other samples (e.g., 10 or 30 wt % TiO_2/G) exhibited the same shape except for the current density magnitude due to the difference in the available active surface area. The anodic process may result from at least two successive electro-oxidations, as is inferred from the two split peaks at approximately −0.1 and +0.2 V (vs Ag/AgCl), respectively.[2] The first peak corresponds to the oxidation of fresh sulfide species, which became available from adsorption, while

DOI: 10.1021/acssuschemeng.5b00277
ACS Sustainable Chem. Eng. 2015, 3, 1764−1770

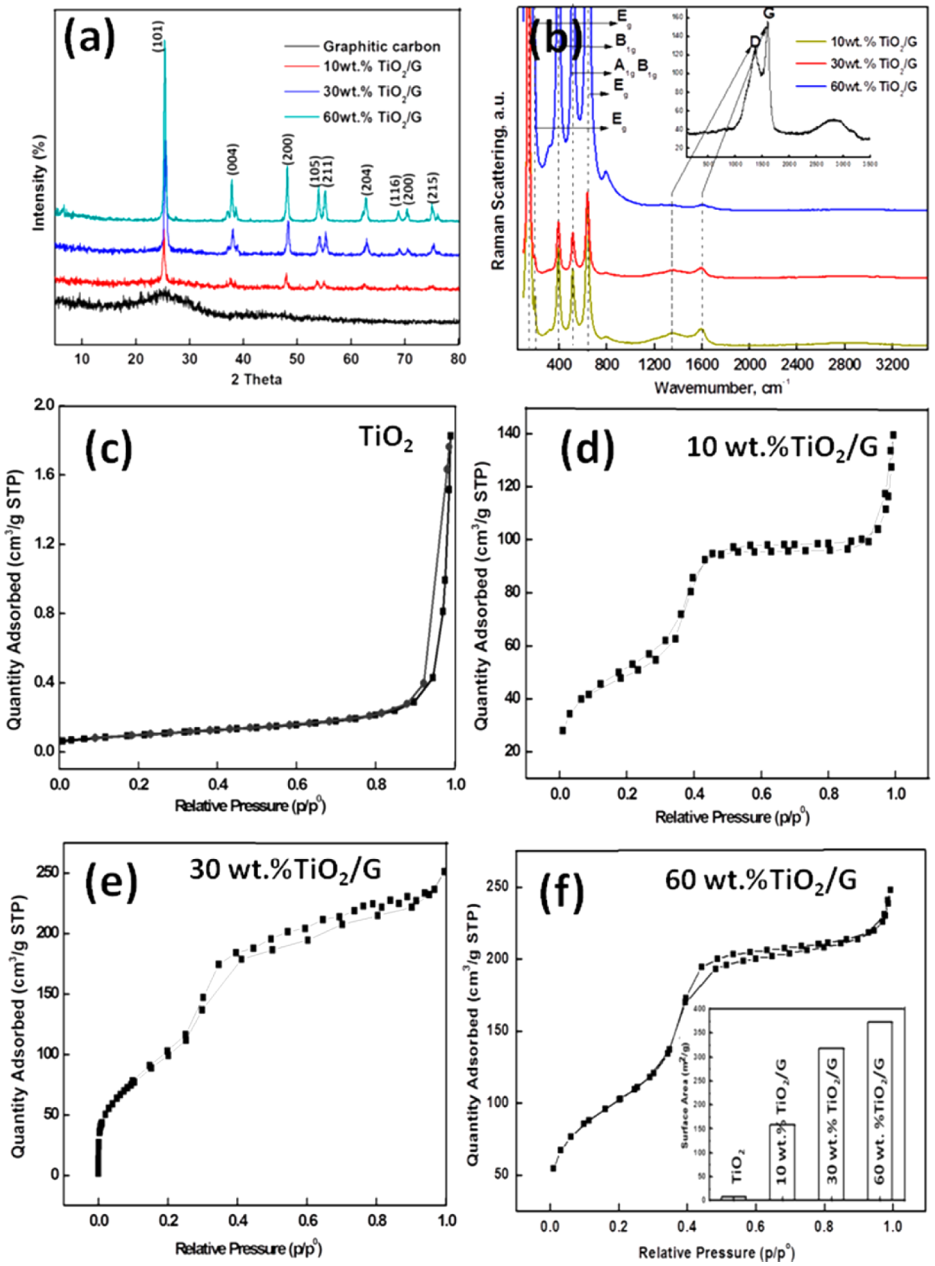

Figure 2. (a) XRD pattern of graphitic carbon and TiO_2/G composite. (b) Raman spectra of TiO_2/G composite; inset represents the spectra of graphitic carbon. Nitrogen adsorption−desorption isotherm loop of (c). TiO_2 (BET surface area is 8 m^2 g^{-1}). (d) 10 wt % TiO_2/G composite (BET surface area is 158.2 m^2 g^{-1}). (e) 30 wt % TiO_2/G composite (BET surface area is 317.8 m^2 g^{-1}). (f) 60 wt % TiO_2/G composite (BET surface area is 372.8 m^2 g^{-1}); inset represents a comparison of BET surface area of the different catalysts.

the second peak seems to arise due to further oxidation of polysulfide species to higher polysulfide.[2] At a high overpotential, the anodic process leads to the ultimate formation of sulfur oxyanions in irreversible manner, as already demonstrated in our previous study eqs 5 and 6.[7]

This novel nanomaterial was applied as a catalyst in the single cell. The polarization and power density curves were obtained with the same mass loading of 2 mg cm^{-2} (Figure 5a) and, thereafter, EIS analysis to gain a Nyquist plot at a single cell voltage of 0.35 V. During all of the analyses, all other conditions remained fixed except for the anode catalyst, so that a difference in single cell performance arose solely from the anodic catalyst. The TiO_2 sample prepared in the absence of the graphitic carbon support showed the worst $I-V$ characteristic, which was expected because TiO_2 itself possesses poor electrical conductivity;[22−24] this was consistently shown as the highest semicircle diameter (charge transfer resistance, R_{ct}) and x-axis intercept value (ohmic resistance, R_{ohm}) in the Nyquist plot, too (Figure 5b). The addition of graphitic carbon (e.g., 10, 30, and 60 wt % TiO_2/G), however, resolved the poor conductivity issue and thus considerably improved cell performances. This result indicated that graphitic carbon, which originated from microalgae, served well as a conductive support by providing effective junctions between TiO_2 and graphitic carbon; as a result, the catalytic activity and conductivity both were ensured. Even more, from comparison to our previous study,[8] it could be seen that the microalgae-originated graphitic carbon supported itself, being used solely without any metal, and showed better catalytic

DOI: 10.1021/acssuschemeng.5b00277
ACS Sustainable Chem. Eng. 2015, 3, 1764−1770

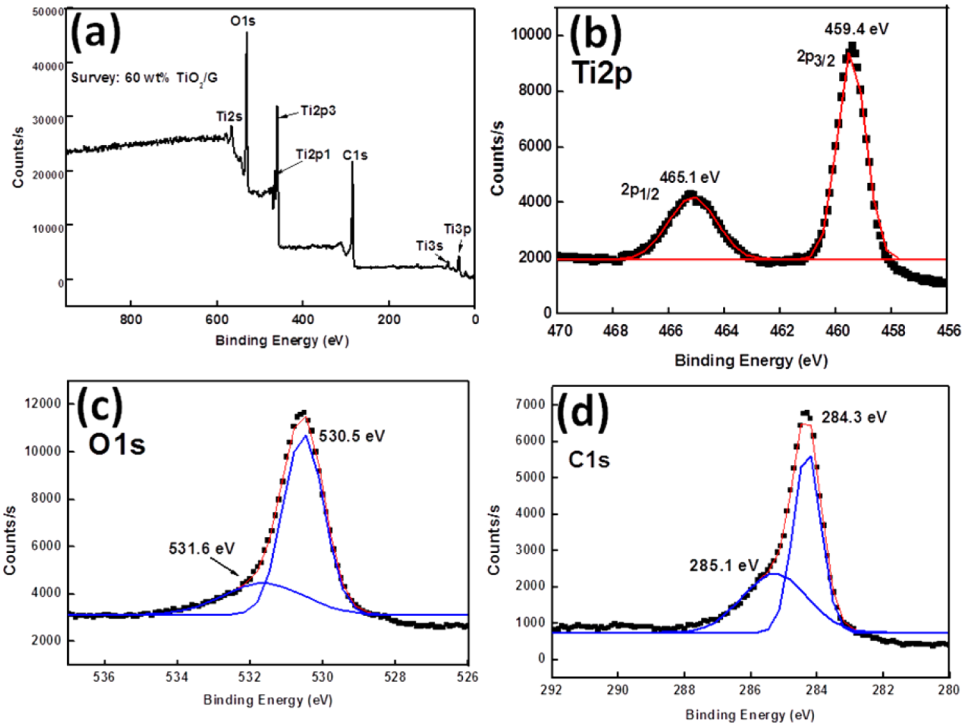

Figure 3. XPS high resolution spectra of 60 wt % TiO2/G: (a) survey plot, (b) Ti 2p, (c) O 1s, and (d) C 1s.

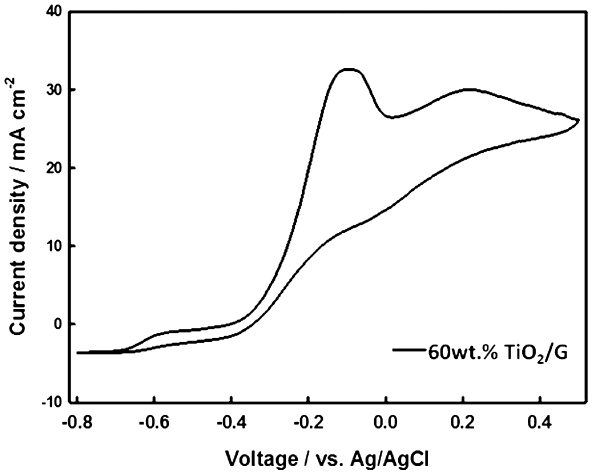

Figure 4. Cyclic voltammograms of 60 wt % TiO_2/G in 1 M Na_2S + 3 M NaOH solution (scan rate, 10 mV s^{-1}; temperature, 20 °C; catalyst loading, 0.15 mg cm^{-2}; rotating speed, 2000 rpm).

activity than a conventional carbon support (namely, Vulcan xc-72).[8] This confirmed its value as a catalyst support.

TiO_2, indeed known as a sulfide-oxidizing catalyst in the Claus process,[25] was found to be similarly active in the electrochemical oxidation of alkaline sulfide, as was clearly exhibited in polarization curves of the graphitic carbon with and without TiO_2. In addition, an increase of TiO_2 loading resulted in better performance, mostly likely because catalytically active sites became more available. This improved performance also supported that TiO_2 can indeed act as an anode catalyst in DASFC. The maximum power densities of DASFC were found to be 26.00, 33.26, and 38.90 mW cm^{-2} for 10, 30, and 60 wt % TiO_2/G, respectively. All the observations from polarization curve were reproduced in the Nyquist plot in which the same trend was observed in terms of R_{ct}.

This study clearly showed that microalgae cells, when being used as a template for nanosized electrocatalyst, well served as an outstanding catalyst support for metal particles, at least in DASFC. Possessing a unique hierarchical structure, it led to a wider active surface on which alkaline sulfide oxidation is catalyzed, and thus, kinetic loss is effectively reduced. Furthermore, many effective junctions between TiO_2 and graphitic carbon, providing a large number of conductive paths along which the derived electrons can successfully be transferred, contributed to minimizing the ohmic loss. This appropriate modification of TiO_2 with microalgae-originated carbon provides a promising and eco-friendly alternative to noble metals as anode catalysts in DASFC.

CONCLUSION

In summary, we have successfully demonstrated a facile biotemplating method to fabricate TiO_2/G composite microstructures. The microalgae used in this work played multiple roles, which acted as low-cost biotemplates to induce unique hierarchical structures and acted as sustainable carbon sources to construct porous matrices by the decomposition of carbonaceous organics. Owing to the unique properties, the TiO_2/G hybrid displayed superior electrochemical performances in DASFC. We believe that this green and economically prepared anodic catalyst is a promising alternative to noble metals in DASFC and also is expected to extend the scope of biotemplated synthesis to other materials for various applications.

EXPERIMENTAL SECTION

Materials. KNO_3, KH_2PO_4, Na_2HPO_4, $MgSO_4.7H_2O$, H_2O_2, and FeNaEDTA were purchased from Samchun Chemical, Korea. $AgNO_3$, $CaCl_2{\cdot}2H_2O$, $ZnSO_4{\cdot}7H_2O$, $MnCl{\cdot}4H_2O$, $CuSO_4{\cdot}5H_2O$, NH_4OH, $Al_2(SO_4)_3{\cdot}18H_2O$, titanium isopropoxide, and ethanol were obtained from Aldrich. $Na_2S{\cdot}5H_2O$ was purchased from Daejung, Korea. All other reagents were purchased from commercial sources and were used without further purification.

DOI: 10.1021/acssuschemeng.5b00277
ACS Sustainable Chem. Eng. 2015, 3, 1764−1770

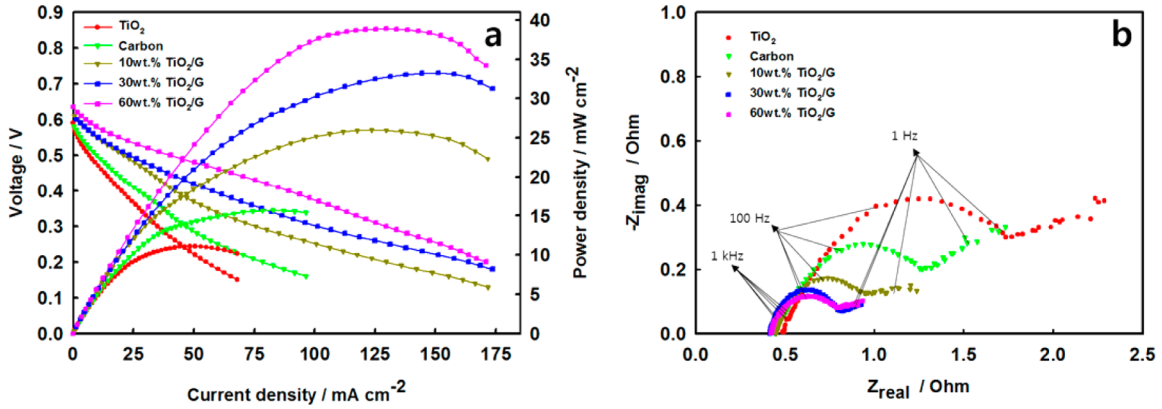

Figure 5. (a) Polarization and power density curve of DASFC with catalysts (anodic fuel, 1 M Na_2S + 3 M NaOH; anodic flow rate, 1 cc min^{-1}; anodic catalyst loading, 2 mg cm^{-2}; cathodic fuel, pure oxygen; cathodic flow rate, 40 cc min^{-1}; cathodic catalyst loading, 3 mg cm^{-2}; cell temperature, 70 °C). (b) Nyquist plot of DASFC with anode catalysts at single cell voltage of 0.35 V.

Methods. *Microalgae Culture.* A locally isolated freshwater microalgae species (*Chlorella* sp. *KR*-1) in South Korea was used for the present study.[16] The cell size was 2−4 μm, and once grown, cell density reached 1.2−1.4 g/L. The culture medium was prepared in tap water and had the following composition (in mM): KNO_3, 3; KH_2PO_4, 5.44; Na_2HPO_4, 1.83; $MgSO_4{\cdot}7H_2O$, 0.20; $CaCl_2{\cdot}2H_2O$, 0.12; FeNaEDTA·$3H_2O$, 0.03; $ZnSO_4{\cdot}7H_2O$, 0.01; $MnCl_2{\cdot}4H_2O$, 0.07; $CuSO_4{\cdot}5H_2O$, 0.07; and $Al_2(SO_4)_3{\cdot}18H_2O$, 0.01. The initial pH of the medium was adjusted to 6.5.

Synthesis of Hierarchical TiO_2/G Hybrid. Microalgae (1.2 g/L) (*Chlorella* sp. KR-1) was concentrated by centrifugation (~4000 rpm) and washed three times in deionized water followed by ethanol to remove the spent medium. The concentrated microalgae cells were dried at room temperature. TiO_2/G composites corresponding to three different weight ratios, TiO_2:G)10:90, 30:70, 60:40 wt % (represented as 10 wt % TiO_2/G, 30 wt % TiO_2/G, and 60 wt % TiO_2/G, respectively) and pure TiO_2 particles were synthesized by means of controlled hydrolysis of titanium isopropoxide followed by heating in an inert atmosphere.[17] Typical synthesis of 10 wt % TiO_2/G was represented as follows: 90 mg of microalgae was dispersed in 100 mL of ethanol and sonicated for 1 min at room temperature; 0.37 mL of titanium(IV) isopropoxide (Aldrich) was added dropwise to the microalgae solution and stirred continuously at 300 rpm. After 30 min of stirring, the hydrolysis of titanium(IV) isopropoxide was facilitated by introducing 0.1 mL of distilled water into the beaker. After 4 h of stirring at room temperature, the resulting precipitate was filtered and washed in ethanol and dried in an oven at 50 °C. The composite was heated to 400 °C (6 h) at argon atmosphere. The obtained brown material was designated as 10 wt % TiO_2/G. For comparison, anatase TiO_2without the addition of microalgae was also prepared using the same experimental conditions. The graphitic carbon was obtained by the pyrolysis of the dried microalgae in argon atmosphere 400 °C (6 h).

Characterization Techniques. The surface morphology of the particles was observed by scanning electron microscopy (FE-SEM, Magellan400).The phase formation and crystallographic state of the sample were collected using powder XRD (Rigaku, model RTP 300 RC) with Cu Kα radiation (λ = 0.154 nm).The nitrogen adsorption−desorption isotherms were measured at −196 °C on a Quantachrome Scientific (Quadrasorb-SI-MP-20) adsorption analyzer. Transmission electron microscopy was analyzed using FE-TEM, JEM-2100F.

Cyclic Voltammetry (CV) Measurement. Cyclic voltammetry was carried out in a conventional three-electrode system equipped with a Pt counter electrode, an Ag/AgCl reference electrode (BAS Co., Ltd.), and a glassy carbon working electrode with surface area is 0.0227 cm^2 (1.7 mm dia., BAS Co., Ltd.). All potentials in this study were referenced to an Ag/AgCl electrode. The working electrodes were prepared by the thin-film method. Six milligrams of the fabricated catalysts was dispersed in 6 mL of IPA/DIW (1/5, v/v) via sonication to obtain homogeneity of the ink, and then 3.5 μL of the ink was dripped onto a glassy carbon electrode to achieve a loading of 0.15 mg cm^{-2}. After drying in an oven overnight, 3.5 μL of Tokuyama ionomer (AS-4, 5 wt %) was also dripped on the catalyst layer to enhance the mechanical strength of the catalyst layer.[11,12] The as-prepared electrodes were then subjected to CV in a potential range from −0.8 to 0.5 V in N_2-purged 1 M Na_2S + 3 M NaOH at a scan rate of 10 mV s^{-1} and at a rotation speed of 2000 rpm with rotating disk electrode (RDE) equipment.

Membrane Electrode Assembly Fabrication and Fuel Cell Setup. Carbon cloth (SCCG-5N, CNL energy) was used as an electrode support and Nafion 117 as a cation exchange membrane (CEM). Before use, the CEM was cleansed in slightly boiled 3 wt % H_2O_2 for 1 h and boiled in 3 M NaOH for 1 h for assigning Na^+ conductivity.[7] The Na^+ modified membrane was then rinsed in deionized water several times. A cathode electrode was a machine-built carbon cloth with 3 mg cm^{-2} of Pt/C (20 wt %, E-Tek). Catalyst inks for the anode were prepared with 30 mg of each sample and 200 μL of 5 wt % Nafion ionomer in 4 mL of IPA/DIW (3/1, v/v). This ink mixture was homogenized by sonication for 1 h and magnetically stirred at 40 °C for several hours, leading to a homogeneous slurry. The slurry was then applied to one side of the anode by brushing to achieve a loading of 2 mg cm^{-2}. After being assembled, a membrane electrode assembly (MEA) comprised of the anode and cathode electrodes and CEM was mounted in a fuel cell device with an active cross-sectional area of 4 cm^2.

Single Cell Tests. For whole tests, the temperature was kept at 70 °C. An alkaline sulfide fuel composed of 1 M Na_2S and 3 M NaOH was fed into the anodic plate channel at a flow rate of 1 cc min^{-1} using a peristaltic pump, while pure oxygen was provided at a flow rate of 40 cc min^{-1} into the cathodic plate channel. After the MEA was activated for 3 h, polarization curves were taken from the results of LSV using a potentiostat (CHI 604C) at a scan rate of 5 mV s^{-1}. EIS analysis was also performed using the potentiostat (CHI 604 C) from 10,000 to 0.05 Hz at cell voltage of 0.35 V with AC amplitude of 5 mV.

AUTHOR INFORMATION

Corresponding Authors

*Tel.: +82 42 350 3926. Fax: +82 42 350 3910. E-mail: jayhlee@kaist.ac.kr.

*Tel.: +82 42 350 3629. Fax: +82 42 350 3610. E-mail: hanj2@kaist.ac.kr.

Author Contributions

Prakash Chandra Sahoo and Kwiyong Kim contributed equally to this work.

Notes

The authors declare no competing financial interest.

ACKNOWLEDGMENTS

This work was supported financially by Advanced Biomass R&D Center (ABC) (ABC-2012053875), Korea Government Ministry

DOI: 10.1021/acssuschemeng.5b00277
ACS Sustainable Chem. Eng. 2015, 3, 1764−1770

of Science, ICT and Future Planning, South Korea. This work is also supported by the National Research Foundation of Korea (NRF) Grant funded by the Korea Government of Ministry of Science, ICT and Future Planning, South Korea (NRF-2012m1a2a2026587).

REFERENCES

(1) Mao, Z.; Anani, A.; White, R. E.; Srinivasan, S.; Appleby, A. J. A modified electrochemical process for the decomposition of hydrogen sulfide in an aqueous alkaline solution. *J. Electrochem. Soc.* **1991**, *138*, 1299−1303.

(2) Anani, A.; Mao, Z.; White, R. E.; Srinivasan, S.; Appleby, A. J. Electrochemical production of hydrogen and sulfur by low-temperature decomposition of hydrogen sulfide in an aqueous alkaline solution. *J. Electrochem. Soc.* **1990**, *137*, 2703−2709.

(3) Liu, M.; He, P.; Luo, J. L.; Sanger, A. R.; Chuang, K. T. Performance of a solid oxide fuel cell utilizing hydrogen sulfide as fuel. *J. Power Sources* **2001**, *94*, 20−25.

(4) He, P.; Liu, M.; Luo, J. L.; Sanger, A. R.; Chuang, K. T. Stabilization of platinum anode catalyst in a H_2S-O_2 solid oxide fuel cell with an intermediate TiO_2 layer. *J. Electrochem. Soc.* **2002**, *149*, A808−814.

(5) Slavov, S. V.; Chuang, K. T.; Sanger, A. R.; Donini, J. C.; Kot, J.; Petrovic, S. A proton-conducting solid state H_2S-O_2 fuel cell. 1. Anode catalysts, and operation at atmospheric pressure and 20−90°C. *Int. J. Hydrogen Energy* **1998**, *23*, 1203−1212.

(6) Chuang, K. T.; Donini, J. C.; Sanger, A. R.; Slavov, S. V. A proton-conducting solid state H_2S-O_2 fuel cell. 2. Production of liquid sulfur at 120−145°C. *Int. J. Hydrogen Energy* **2000**, *25*, 887−894.

(7) Kim, K.; Han, J.-I. Performance of direct alkaline sulfide fuel cell without sulfur deposition on anode. *Int. J. Hydrogen Energy* **2014**, *39*, 7142−7146.

(8) Kim, K.; Son, J.; Han, J.-I. Metal sulfides as anode catalysts in direct alkaline sulfide fuel cell. *Int. J. Hydrogen Energy* **2014**, *39*, 10493−10497.

(9) Kim, K.; Han, J.-I. Heteropolyacids as anode catalysts in direct alkaline sulfide fuel cell. *Int. J. Hydrogen Energy* **2015**, *40*, 2979−2983.

(10) Kim, K.; Kim, H.-T.; Han, J.-I. Compatibility of platinum with alkaline sulfide fuel: Effectiveness and stability of platinum as an anode catalyst in direct alkaline sulfide fuel cell. *Int. J. Hydrogen Energy* **2015**, *40*, 4141−4145.

(11) Kim, K.; Han, J.-I. Carbon supported bimetallic Pd−Co catalysts for alkaline sulfide oxidation in direct alkaline sulfide fuel cell. *Int. J. Hydrogen Energy* **2015**, *40*, 4567−4572.

(12) Kim, K.; Han, J.-I. Carbon-supported bimetallic Pd−Ir catalysts for alkaline sulfide oxidation in direct alkaline sulfide fuel cell. *J. Appl. Electrochem.* **2015**, *45*, 533−539.

(13) Qiao, Y.; Li, C. M. Nanostructured catalysts in fuel cells. *J. Mater. Chem.* **2011**, *21*, 4027−4036.

(14) Le, Y.; Guo, D.; Cheng, B.; Yu, J. Bio-template-assisted synthesis of hierarchically hollow SiO2 microtubes and their enhanced formaldehyde adsorption performance. *Appl. Surf. Sci.* **2013**, *274*, 110−116.

(15) Shim, H.; Lim, A.; Kim, J.; Jang, E.; Seo, S.; Lee, G.; Kim, T. D.; Kim, D. Scalable One-pot Bacteria-templating Synthesis Route toward Hierarchical, Porous-Co3O4Superstructures for Supercapacitor Electrodes. *Sci. Rep.* **2013**, DOI: 10.1038/srep02325.

(16) Hwang, T.; Park, S.; Oh, Y.; Rashid, N.; Han, J. I. Harvesting of Chlorella sp. KR-1 using a cross-flow membrane filtration system equipped with an anti-fouling membrane. *Bioresour. Technol.* **2013**, *139*, 379−282.

(17) Hemalatha, K.; Prakash, A. S.; Guruprakash, K.; Jayakumar, M. TiO_2coated carbon nanotubes for electrochemical energy storage. *J. Mater. Chem. A* **2014**, *2*, 1757−1766.

(18) Shao, X.; Lu, W.; Zhang, R.; Pan, F. Enhanced photo catalytic activity ofTiO_2-C hybrid aerogels for methylene blue degradation. *Sci. Rep.* **2013**, DOI: 10.1038/srep03018.

(19) Yang, Z.; Du, G.; Guo, Z.; Yu, X.; Chen, Z.; Guo, T.; Liu, H. TiO_2(B)@carbon composite nanowires as anode for lithium ion batteries with enhanced reversible capacity and cyclic performance. *J. Mater. Chem.* **2011**, *21*, 8591−8596.

(20) XPS database. http://www.lasurface.com/database/elementxps.php (accessed May, 2015).

(21) Ohtsu, N.; Masahashi, N.; Mizukoshi, Y.; Wagatsuma, K. Hydrocarbon decomposition on a hydrophilic TiO_2 surface by UV irradiation: spectral and quantitative analysis using in-situ XPS technique. *Langmuir* **2009**, *25*, 11586−11591.

(22) Qiao, Y.; Bao, S. J.; Li, C. M.; Cui, X.; Lu, Z.; Guo, J. Nanostructured Polyaniline/Titanium Dioxide Composite Anode for Microbial Fuel Cells. *ACS Nano* **2008**, *2*, 113−119.

(23) Zhang, X.; Suresh Kumar, P.; Aravindan, V.; Liu, H.; Sundaramurthy, J.; Mhaisalkar, S. G.; Duong, H.; Ramakrishna, S.; Madhavi, S. Electrospun TiO_2−Graphene Composite Nanofibers as a Highly Durable Insertion Anode for Lithium Ion Batteries. *J. Phys. Chem. C* **2012**, *116*, 14780−14788.

(24) Zhao, C.; Wang, W.; Sun, D.; Wang, X.; Zhang, J.; Zhu, J. Nanostructured Graphene/TiO_2Hybrids as High-Performance Anodes for Microbial Fuel Cells. *Chem. - Eur. J.* **2014**, *20*, 7091−7097.

(25) Davydov, A. A.; Marshneva, V. L.; Shepotko, M. L. Metal oxides in hydrogen sulfide oxidation by oxygen and sulfur dioxide: I. The comparison study of the catalytic activity. Mechanism of the interaction between H_2S and SO_2 on some oxides. *Appl. Catal., A* **2003**, *244*, 93−100.

DOI: 10.1021/acssuschemeng.5b00277
ACS Sustainable Chem. Eng. 2015, 3, 1764−1770